The 2nd Joint International Conference on Multibody System Dynamics
May 29–June 1, 2012, Stuttgart, Germany

Numerical Experiments with the Painlevé Paradox: Rigid Body vs. Compliant Contact

T. Preclik*, **U. Rüde***

* Chair for System Simulation
University of Erlangen-Nürnberg
Cauerstr. 11, 91058 Erlangen, Germany
[tobias.preclik, ulrich.ruede]@informatik.uni-erlangen.de

ABSTRACT

The existence and (non-)uniqueness of rigid multibody problems with impact, contact and friction is discussed by means of the renowned Painlevé paradox. Different approaches to solve such contact problems, their pros and cons and their connections are discussed.

1 INTRODUCTION

The question of solution existence and uniqueness of rigid multibody dynamics with impact and frictional contacts has a long history and was and still is subject to controversial discussions. Paul Painlevé published in 1895 a simple example reputedly demonstrating the absence or the multiplicity of solutions in the case of dry Coulomb friction [5] depending on how the initial conditions are chosen. Coulomb friction just like impact situations possibly do not have instantaneous solutions if one only considers contact reaction *forces* as solutions. Collisions as well as Coulomb friction can produce velocity jumps in the solution. David Stewart resolved the paradox by ensuring that impulsive reactions are allowed by the mathematical formulation [11]. Stewart presented a linear complementarity problem (LCP) formulation which can provably be solved by the Lemke algorithm. Though this is a convenient theoretical result the Lemke algorithm has exponential complexity in the worst case. However, it typically performs much better taking only n pivot steps, where n is the problem size. Since a pivot step generally has quadratic complexity the Lemke algorithm needs $\mathcal{O}(n^3)$ operations on average. Nevertheless, the algorithm in practice does not perform well on problems with several hundred unknowns. Instead different variants of fixed-point iterations are applied nowadays reminding of the well-known successive over-relaxation or Jacobi methods. The convergence of such methods can deteriorate or even fail if multiple solutions exist. Thus to improve the performance of such methods it is important to understand the sources of solution non-uniqueness in order to be able to cope with them.

2 FORCE-ACCELERATION CONTACT PROBLEMS

Painlevé's paradox consists of an inclined rod directly in contact with the ground plane subject to gravity. The rod can be described by the position of its center of gravity $\boldsymbol{q} = (q_x, q_y)^T$ and its orientation φ. The equations of motions then read

$$\begin{pmatrix} m & & \\ & m & \\ & & I \end{pmatrix} \begin{pmatrix} \ddot{q}_x \\ \ddot{q}_y \\ \ddot{\varphi} \end{pmatrix} = \begin{pmatrix} \lambda_t + f_x \\ \lambda_n + f_y \\ \frac{l}{2}\lambda_t \sin(\varphi) + \frac{l}{2}\lambda_n \sin(\varphi - \frac{\pi}{2}) + \tau \end{pmatrix} = \begin{pmatrix} f_x \\ f_y \\ \tau \end{pmatrix} + \mathbf{J}^T \boldsymbol{\lambda}, \tag{1}$$

where l is the length of the rod, m is the mass, I is the moment of inertia, $\boldsymbol{f} = (f_x, f_y)^T$ are external forces, τ is an external torque, $\mathbf{J}$ is the Jacobian matrix, $\boldsymbol{\lambda} = (\lambda_n, \lambda_t)^T$ are the contact reactions and where the orientation φ coincides with the angle between ground and rod (measured in counterclockwise direction). Fig. 1 illustrates the setup.

The frictional contact constraints are formulated in terms of the gap function $\boldsymbol{g}$. The gap function returns for a pair of points initially corresponding to surface points of two bodies with minimal distance, the current

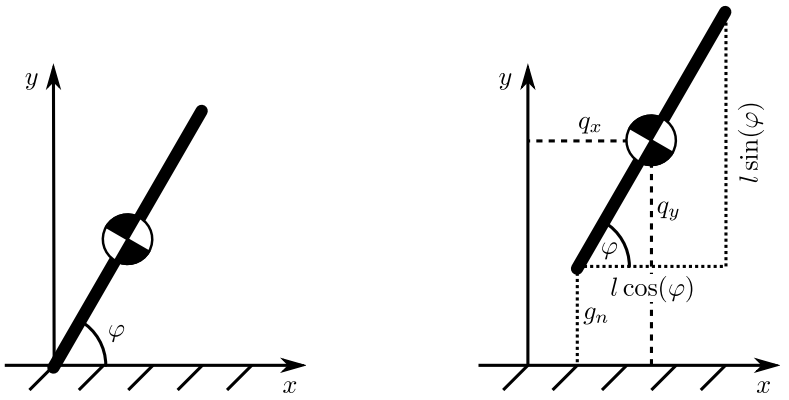

(a) The actual setup with the contact at the origin.

(b) An alternative setup for illustrating the variables.

Figure 1: The general setup of the Painlevé's paradox.

distance in normal and tangential direction. Assuming the rod initially contacts the ground at the origin, the gap function is

$$\boldsymbol{g} = \begin{pmatrix} g_n \\ g_t \end{pmatrix} = \begin{pmatrix} q_y - \frac{l}{2}\sin(\varphi) \\ q_x - \frac{l}{2}\cos(\varphi) \end{pmatrix}. \tag{2}$$

Differentiating once w.r.t. time leads to

$$\dot{\boldsymbol{g}} = \begin{pmatrix} \frac{\partial \boldsymbol{g}}{\partial q_x} & \frac{\partial \boldsymbol{g}}{\partial q_y} & \frac{\partial \boldsymbol{g}}{\partial \varphi} \end{pmatrix} \begin{pmatrix} \dot{\boldsymbol{q}} \\ \dot{\varphi} \end{pmatrix} = \begin{pmatrix} 0 & 1 & -\frac{l}{2}\cos(\varphi) \\ 1 & 0 & \frac{l}{2}\sin(\varphi) \end{pmatrix} \begin{pmatrix} \boldsymbol{v} \\ \omega \end{pmatrix} = \mathbf{J} \begin{pmatrix} \boldsymbol{v} \\ \omega \end{pmatrix}, \tag{3}$$

where $\mathbf{J}$ is the constraint Jacobian, $\boldsymbol{v} = (v_x, v_y)^T$ is the translational velocity and ω the angular velocity of the rod. Differentiating a second time results in

$$\begin{aligned} \ddot{\boldsymbol{g}} &= \begin{pmatrix} \ddot{q}_y + \frac{l}{2}\sin(\varphi)\dot{\varphi}^2 - \frac{l}{2}\cos(\varphi)\ddot{\varphi} \\ \ddot{q}_x + \frac{l}{2}\cos(\varphi)\dot{\varphi}^2 + \frac{l}{2}\sin(\varphi)\ddot{\varphi} \end{pmatrix} \\ &= \begin{pmatrix} \frac{1}{m} + \frac{l^2}{4I}\cos^2(\varphi) & -\frac{l^2}{4I}\sin(\varphi)\cos(\varphi) \\ -\frac{l^2}{4I}\sin(\varphi)\cos(\varphi) & \frac{1}{m} + \frac{l^2}{4I}\sin^2(\varphi) \end{pmatrix} \begin{pmatrix} \lambda_n \\ \lambda_t \end{pmatrix} + \begin{pmatrix} \frac{f_y}{m} + \frac{l}{2}\sin(\varphi)\omega^2 - \frac{l}{2}\cos(\varphi)\frac{\tau}{I} \\ \frac{f_x}{m} + \frac{l}{2}\cos(\varphi)\omega^2 + \frac{l}{2}\sin(\varphi)\frac{\tau}{I} \end{pmatrix}. \end{aligned} \tag{4}$$

The Signorini contact condition then states that

$$g_n \geq 0 \perp \lambda_n \geq 0. \tag{5}$$

It requires that the gap and the normal reaction is non-negative and that the normal reaction is non-zero only if the gap is zero. There are three possibilities now: Either the current gap is greater than zero ($g_n > 0$) then the complementarity condition fixes $\lambda_n = 0$. The second possibility is that the gap is exactly zero ($g_n = 0$) then $\lambda_n \geq 0$ but the actual normal reaction cannot be determined. In the third case where the gap is negative ($g_n < 0$) the constraint is clearly violated and no normal reaction force (nor impulse) can be determined which would result in a feasible solution in the immediate future. To determine the normal reaction in the second case the Signorini contact condition must be replaced by a corresponding constraint for the approach velocity $\dot{g}_n$:

$$\dot{g}_n \geq 0 \perp \lambda_n \geq 0. \tag{6}$$

Again three cases exist: If $\dot{g}_n > 0$ then the contact breaks and no contact reaction is present. If $\dot{g}_n < 0$ then a *collision* occurs and penetration cannot be avoided no matter which normal reaction force is applied. Instead one would need an impulse to produce a discontinuity in the approach velocity so that no interpenetration occurs in the immediate future. In order to continue the discussion with a force-acceleration formulation we exclude this case as we also exclude cases where the gap is already violated. The third case applies if $\dot{g}_n = 0$, then the normal reaction is known to be non-negative due to the complementarity condition but the

magnitude cannot be determined from the condition. Thus the complementarity condition again has to be replaced this time by a condition on the approach acceleration:

$$\ddot{g}_n \geq 0 \perp \lambda_n \geq 0. \tag{7}$$

From this condition one can finally deduce the value of the normal reaction force (unless the complementarity condition has no solution).

If the contact is closed, i.e. $g_n = 0$ Coulomb friction acts. Coulomb friction in turn can be in two states. In case the slip (the relative tangential velocity) is zero ($\dot{g}_t = 0$) the contact is in the static case and the frictional reactions are allowed to be less than or equal to the coefficient of friction μ times the normal reaction λ_n in magnitude. If the slip is non-zero ($\dot{g}_t \neq 0$) then the contact is in the dynamic state and the frictional reaction directly opposes the slip and is at its limits (i.e. has magnitude $\mu\lambda_n$). These conditions can be combined in a (non-standard) complementarity condition:

$$\dot{g}_t \gtreqless 0 \perp -\mu\lambda_n \leq \lambda_t \leq \mu\lambda_n. \tag{8}$$

This uncommon notation has to be understood as follows: If there is no slip ($\dot{g}_t = 0$) then the frictional reaction force must be within its limits, if $\dot{g}_t < 0$ then friction must be at its upper bound $\mu\lambda_n$ and if $\dot{g}_t > 0$ then friction must be at its lower bound $-\mu\lambda_n$. As before some of these cases determine the value of λ_t. Here, if the slip $\dot{g}_t$ is non-zero (and thus the contact is dynamic) then $\lambda_t = \pm\mu\lambda_n$. In the static case where there is no slip ($\dot{g}_t = 0$) as before λ_t cannot be pinpointed and the complementarity condition is replaced by the corresponding condition on the relative tangential acceleration $\ddot{g}_t$:

$$\ddot{g}_t \gtreqless 0 \perp -\mu\lambda_n \leq \lambda_t \leq \mu\lambda_n. \tag{9}$$

And as in the case of the normal reaction force, the friction force can finally be deduced from that condition (unless the complementarity condition has no solution).

2.1 Solution Non-Existence

First we will demonstrate that force-acceleration based approaches as presented above can fail to have solutions even if no collision and constraint violation is present. Therefore we choose the following initial conditions: The rod is directly in contact ($g_n = 0$) and no impact occurs ($\dot{g}_n = 0$). Thus we choose $\varphi \in (0; \frac{1}{2}\pi)$, $q_x = \frac{l}{2}\cos(\varphi)$, $q_y = \frac{l}{2}\sin(\varphi)$, $\omega = 0$ and $v_y = 0$. It is also pressed against the ground for example due to gravity $g > 0$ and thus we choose $f_x = 0$, $f_y = -mg$ and $\tau = 0$. Furthermore, the rod is sliding to the left ($\dot{g}_t < 0$) and thus we choose $v_x < 0$. The sliding allows us to determine the frictional reaction force λ_t to be $\mu\lambda_n$ leading together with Eq. (7) and Eq. (4) to

$$\left(\frac{1}{m} + \frac{l^2}{4I}\cos^2(\varphi) - \mu\frac{l^2}{4I}\sin(\varphi)\cos(\varphi)\right)\lambda_n + \left(\frac{f_y}{m} + \frac{l}{2}\sin(\varphi)\omega^2 - \frac{l}{2}\cos(\varphi)\frac{\tau}{I}\right) \geq 0 \perp \lambda_n \geq 0. \tag{10}$$

This setup closely resembles a piece of chalk pressed against the board at an angle φ and sliding to the left. This scalar complementarity condition is of the type

$$Ax - b \geq 0 \perp x \geq 0 \tag{11}$$

and its solvability depends on the signs of A and b. If $A > 0$ then the complementarity condition always has a solution since if $b \geq 0$ then $x = \frac{b}{A} \geq 0$ and $Ax - b = 0$ and if $b < 0$ then $x = 0$ and $Ax - b = -b > 0$. However, if $A < 0$ then the complementarity condition only has solutions if $b \leq 0$ since then $x = 0$ solves the complementarity condition. But if $b > 0$ then $Ax - b < 0$ for any $x \geq 0$. For the above initial conditions $b = -(\frac{f_y}{m} + \frac{l}{2}\sin(\varphi)\omega^2 - \frac{l}{2}\cos(\varphi)\frac{\tau}{I}) = g > 0$ and the system is thus unsolvable for $A < 0$. If the rod is a perfectly slender rod then the moment of inertia is $\frac{l^2 m}{12}$ and the sign of A no longer depends on m and l but only on μ. If we choose for example $\mu = \frac{3}{2}$ and $\varphi = \frac{\pi}{3}$ then A becomes negative and the complementarity condition has no solution. For details refer to [8].

2.2 Solution Non-Uniqueness

When choosing $A < 0$ and $b < 0$ then the complementarity condition Eq. (11) actually has two solutions: One of them being $x = 0$ since $Ax - b = -b > 0$ and the other one being $x = \frac{b}{A} > 0$ since $Ax - b = 0$. In

terms of mechanics this means that there are two possible force solutions where one of them has no contact reaction force ($x = \lambda_n = \lambda_t = 0$) and the contact breaks and the other is a (closed) dynamic contact.

To ensure $b < 0$ we choose a non-zero torque τ in contrast to the case before:

$$\begin{aligned} b &= -(\frac{f_y}{m} + \frac{l}{2}\sin(\varphi)\omega^2 - \frac{l}{2}\cos(\varphi)\frac{\tau}{I}) \overset{!}{<} 0 \\ \tau &< \frac{2f_y I}{ml\cos(\varphi)} \end{aligned} \tag{12}$$

Note that it is still guaranteed that $\dot{g}_n = 0$ since we still assume $v_y = \omega = 0$. This way we obtain the same complementarity condition as in Eq. (10). The same non-uniqueness appears if we suitably choose ω but in that case we also have to choose $v_y = \frac{l}{2}\cos(\varphi)\omega$ so that $\dot{g}_n = 0$. For unitless $\tau = \frac{2f_y I}{ml\cos(\varphi)} - 1$, $l = 2$, $m = 1$, $I = \frac{l^2 m}{12}$, $g = 1$ and $v_x = -1$ we obtain the solutions $\boldsymbol{\lambda}_1 = (0,0)^T$ (opening) and $\boldsymbol{\lambda}_2 \approx (7.5545, 11.3317)^T$ (dynamic).

3 INSTANTANEOUS IMPULSE-VELOCITY CONTACT PROBLEMS

As remarked earlier the force-acceleration based formulation has the drawback that it cannot deal with impulsive reactions. This immediately excludes collision situations. However, the Painlevé example is constructed such that no collision occurs and nevertheless no solution exists. This indicates that Coulomb friction potentially requires impulsive reactions. This is often also referred to as an impact without collision [4].

Impulses $\boldsymbol{\Lambda}$ introduce discontinuities in the translational and angular velocity solutions. Consequently the state variables can no longer be differentiated. But one still can solve the instantaneous impulse-velocity problem

$$\begin{pmatrix} m & & \\ & m & \\ & & I \end{pmatrix} \begin{pmatrix} \delta v_x \\ \delta v_y \\ \delta\omega \end{pmatrix} = \mathbf{J}^T \boldsymbol{\Lambda}, \tag{13}$$

where $\delta\boldsymbol{v} = \boldsymbol{v}^+ - \boldsymbol{v}^-$ and $\delta\omega = \omega^+ - \omega^-$. The constraints still originate from the Signorini contact condition, which still needs to be differentiated if the contact is closed because impulses do not instantaneously change positions. The corresponding constraint of the approach velocity now reads

$$\dot{g}_n^+ = \mathbf{J}_{n*} \begin{pmatrix} \boldsymbol{v}^+ \\ \omega^+ \end{pmatrix} = \mathbf{J}_{n*} \begin{pmatrix} \boldsymbol{v}^- \\ \omega^- \end{pmatrix} + \mathbf{J}_{n*}\mathbf{M}^{-1}\mathbf{J}^T\boldsymbol{\Lambda} \geq 0 \perp \Lambda_n \geq 0. \tag{14}$$

The Coulomb friction constraints are already velocity constraints and now read

$$\dot{g}_t^+ = \mathbf{J}_{t*} \begin{pmatrix} \boldsymbol{v}^+ \\ \omega^+ \end{pmatrix} = \mathbf{J}_{t*} \begin{pmatrix} \boldsymbol{v}^- \\ \omega^- \end{pmatrix} + \mathbf{J}_{t*}\mathbf{M}^{-1}\mathbf{J}^T\boldsymbol{\Lambda} \gtreqless 0 \perp -\mu\Lambda_n \leq \Lambda_t \leq \mu\Lambda_n. \tag{15}$$

Eq. (14) and Eq. (15) can be combined into a single LCP and Eq. (15) can also be broken up into standard linear complementarity conditions.

3.1 Solution Non-Existence Continued

The resulting LCP for the inconsistent Painlevé paradox from Sec. 2.1 has the obvious solution $\boldsymbol{\Lambda}_1 = (0,0)^T$ - since $v_y = 0$ there is no need for a normal impulse and consequently no frictional impulse can occur. This solution would obviously have no effect on the solvability of a subsequent force-acceleration LCP since the state variables won't change. But for the initial conditions presented above there exists another (impulsive) solution which turns the dynamic, closed (sliding) contact into a static, closed (sticking) contact (slip-stick transition). The solution is the same as the solution of the corresponding linear system of equations $\boldsymbol{\Lambda}_2 \approx (0.3248, 0.4375)^T$.

Fig. 2 presents the solution space of the LCP with the initial conditions as in Sec. 2.1. The precise values are $m = 1, l = 2, I = \frac{l^2 m}{12}, \varphi = \frac{\pi}{3}, \mu = \frac{3}{2}, g = 1$ and $v_x = -1$. The dark blue line are the solutions of the Signorini contact condition Eq. (14) for all possible frictional values and the light blue line are the solutions of the Coulomb friction condition Eq. (15) for all feasible normal reactions. Intersections mark solutions of the overall LCP. The boundary of the friction cone is marked by black lines. Furthermore the isolines of the velocity energy function are plotted in yellow to red colors. The green arrow denotes the steepest descent direction at the trivial solution. The other solution is the solution with the minimum energy and thus has no descent direction.

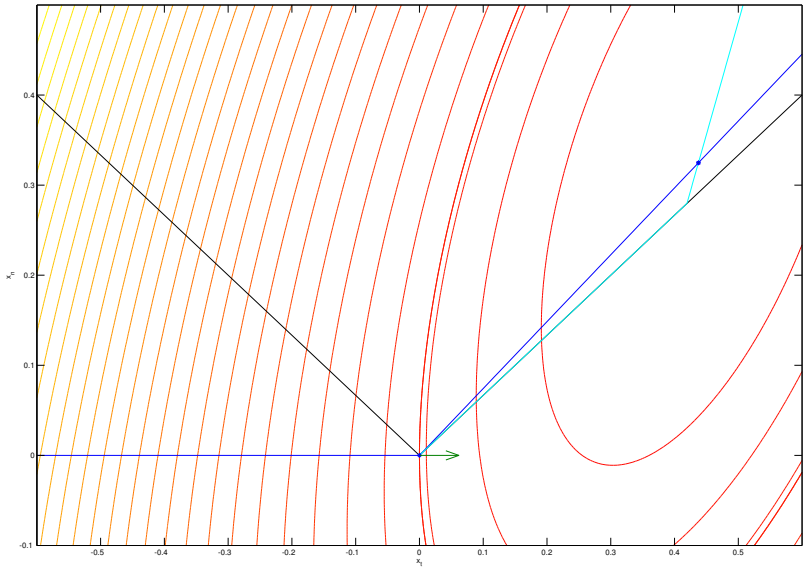

Figure 2: Solution space of the instantaneous impulse-velocity LCP for the setup with no force solutions from Sec. 2.1.

3.2 Solution Non-Uniqueness Continued

The example in Sec. 2.2 demonstrates that force-acceleration contact problems can have multiple solutions. This belies that there can be further impulsive solutions not accessible to the force-acceleration approach. By calculating the solutions of the instantaneous impulse-velocity contact problem one can reveal those. Since the setups with no and multiple solutions only differ in terms of the applied torque τ, the instantaneous impulse-velocity contact problems are in fact the same and thus the non-unique setup also has the same impulsive solutions: $\mathbf{\Lambda}_2 \approx (0.3248, 0.4375)^T$ turning the contact into a static contact besides the already known opening contact reaction $\mathbf{\Lambda}_1 = (0, 0)^T$.

4 TIME-STEPPING SCHEMES

In Sec. 2 instantaneous problems were constructed and *forces* were solved for so that the resulting *accelerations* will not violate constraints when integrated for the immediate future. The need for impulsive solutions became clear in order to guarantee solution existence. In Sec. 3 an instantaneous impulse-velocity LCP was presented which can be used to compute impulsive solutions but the coupling with the force-acceleration LCP is cumbersome not knowing which impulse solutions might lead to a solvable force-acceleration LCP. However, both approaches can be combined in a single complementarity formulation allowing for impulses as well as forces. The idea is to time-discretize the differential equations and require the Signorini and frictional constraints to be met at the end of the time step.

Typically the differential equations are discretized using a semi-implicit Euler scheme where positions are

integrated implicitly

$$\begin{pmatrix} \tilde{q}_x' \\ \tilde{q}_y' \\ \tilde{\varphi}' \end{pmatrix} = \begin{pmatrix} \tilde{q}_x \\ \tilde{q}_y \\ \tilde{\varphi} \end{pmatrix} + \delta t \begin{pmatrix} \tilde{v}_x' \\ \tilde{v}_y' \\ \tilde{\omega}' \end{pmatrix} \tag{16}$$

and velocities are integrated explicitly

$$\begin{pmatrix} \tilde{v}_x' \\ \tilde{v}_y' \\ \tilde{\omega}' \end{pmatrix} = \begin{pmatrix} \tilde{v}_x \\ \tilde{v}_y \\ \tilde{\omega} \end{pmatrix} + \delta t \begin{pmatrix} m & & \\ & m & \\ & & \tilde{I} \end{pmatrix}^{-1} \begin{pmatrix} \tilde{\lambda}_t + \tilde{f}_x \\ \tilde{\lambda}_n + \tilde{f}_y \\ \frac{l}{2}(\tilde{\lambda}_t \sin(\tilde{\varphi}) - \tilde{\lambda}_n \cos(\tilde{\varphi})) + \tilde{\tau} \end{pmatrix} = \begin{pmatrix} \tilde{\boldsymbol{v}} \\ \tilde{\omega} \end{pmatrix} + \delta t \tilde{\mathbf{M}}^{-1} \left(\begin{pmatrix} \tilde{\boldsymbol{f}} \\ \tilde{\tau} \end{pmatrix} + \tilde{\mathbf{J}}^T \tilde{\boldsymbol{\lambda}} \right), \tag{17}$$

Note that ˜ indicates time-discretized quantities and $'$ indicates quantities at the end of the time step. We can now use a Taylor expansion of Eq. (2) to estimate the gap $\tilde{g}_n'$ and slip $\tilde{\dot{g}}_t'$

$$\tilde{g}_n' = \tilde{g}_n + \delta t \tilde{\dot{g}}_n' = \tilde{g}_n + \delta t \tilde{\mathbf{J}}_{n*} \begin{pmatrix} \tilde{\boldsymbol{v}}' \\ \tilde{\omega}' \end{pmatrix} + \mathcal{O}(\delta t^2) \tag{18a}$$

$$\tilde{\dot{g}}_t' = \tilde{\mathbf{J}}_{t*} \begin{pmatrix} \tilde{\boldsymbol{v}}' \\ \tilde{\omega}' \end{pmatrix} \tag{18b}$$

at the end of the time step. The complementarity conditions now read

$$\frac{\tilde{g}_n}{\delta t} + \tilde{\mathbf{J}}_{n*} \tilde{\mathbf{M}}^{-1} \tilde{\mathbf{J}}^T \delta t \tilde{\boldsymbol{\lambda}} + \tilde{\mathbf{J}}_{n*} \left(\begin{pmatrix} \tilde{\boldsymbol{v}} \\ \tilde{\omega} \end{pmatrix} + \delta t \tilde{\mathbf{M}}^{-1} \begin{pmatrix} \tilde{\boldsymbol{f}} \\ \tilde{\tau} \end{pmatrix} \right) \geq 0 \perp \tilde{\lambda}_n \geq 0 \tag{19a}$$

$$\tilde{\mathbf{J}}_{t*} \tilde{\mathbf{M}}^{-1} \tilde{\mathbf{J}}^T \delta t \tilde{\boldsymbol{\lambda}} + \tilde{\mathbf{J}}_{t*} \left(\begin{pmatrix} \tilde{\boldsymbol{v}} \\ \tilde{\omega} \end{pmatrix} + \delta t \tilde{\mathbf{M}}^{-1} \begin{pmatrix} \tilde{\boldsymbol{f}} \\ \tilde{\tau} \end{pmatrix} \right) \gtreqless 0 \perp -\tilde{\mu} \tilde{\lambda}_n \leq \tilde{\lambda}_t \leq \tilde{\mu} \tilde{\lambda}_n, \tag{19b}$$

where the Signorini contact condition was scaled by $\frac{1}{\delta t}$. When neglecting the initial gaps $\tilde{g}_n$ this complementarity problem is solvable as reviewed in [11] since it can be reformulated in a standard LCP whose system matrix is copositive. Then the LCP is known to have solutions and the Lemke algorithm can find them.

4.1 Solution Non-Existence Continued

Fig. 3(a) illustrates the solution space of this LCP for the inconsistent Painlevé problem presented in Sec. 2.1 and Sec. 3.1 for a time step $\delta t = 0.01$. The LCP has a single solution at $\delta t \tilde{\boldsymbol{\lambda}} \approx (0.3329, 0.4407)^T$. In comparison to the impulse-velocity solutions of Sec. 3.1 the trivial solution vanished and $\boldsymbol{\Lambda}_2 \approx (0.3248, 0.4375)^T$ differs by $\mathcal{O}(\delta t)$ as can be confirmed numerically by reducing δt and monitoring the difference.

4.2 Solution Non-Uniqueness Continued

Let us try to repeat the calculations for the setup with non-unique solutions of Sec. 2.2. The right-hand side now reduces to $b = -\delta t \tilde{\mathbf{J}}_{n*} \tilde{\mathbf{M}}^{-1} \begin{pmatrix} \tilde{\boldsymbol{f}} \\ \tilde{\tau} \end{pmatrix} = -\delta t (\frac{\tilde{f}_y}{m} - \frac{l}{2} \cos(\tilde{\varphi}) \frac{\tilde{\tau}}{\tilde{I}})$ since the collision-freeness guarantees that $\tilde{\mathbf{J}}_{n*} \begin{pmatrix} \tilde{\boldsymbol{v}} \\ \tilde{\omega} \end{pmatrix} = 0$. In contrast to Sec. 2.2 this term is independent of $\tilde{\omega}$ but one can still use the torque $\tilde{\tau}$ to demonstrate the non-uniqueness in case $b < 0$ as before:

$$\begin{aligned} b &= -\delta t (\frac{\tilde{f}_y}{m} - \frac{l}{2} \cos(\tilde{\varphi}) \frac{\tilde{\tau}}{\tilde{I}}) \overset{!}{<} 0 \\ \tilde{\tau} &< \frac{2 \tilde{f}_y \tilde{I}}{m l \cos(\tilde{\varphi})} \end{aligned} \tag{20}$$

Fig. 3(b) shows the solution space of the setup from Sec. 2.2 with $\tilde{\tau} = \frac{2\tilde{f}_y\tilde{I}}{ml\cos(\tilde{\varphi})} - 1$. The LCP has three solutions in contrast to the force-acceleration LCP, which only has the solutions for an opening and a dynamic, closed contact. The solution turning the contact into a static contact is impulsive. The solutions are $\delta t\tilde{\boldsymbol{\lambda}}_1 = (0,0)^T$ (opening), $\delta t\tilde{\boldsymbol{\lambda}}_2 \approx (0.0755, 0.1133)^T$ (dynamic) and $\delta t\tilde{\boldsymbol{\lambda}}_3 \approx (0.3266, 0.4516)^T$ (static), where solutions 1 and 2 match the solutions computed by the force-acceleration LCP in Sec. 2.2 and solution 3 matches the solution $\boldsymbol{\Lambda}_2$ computed by the instantaneous impulse-velocity LCP in Sec. 3.2 up to $\mathcal{O}(\delta t)$ as can be confirmed numerically by reducing δt and monitoring the difference. Decreasing δt results in $\delta t\tilde{\boldsymbol{\lambda}}_2$ converging towards $(0,0)^T$ and $\delta t\tilde{\boldsymbol{\lambda}}_3$ converges towards $\boldsymbol{\Lambda}_2$.

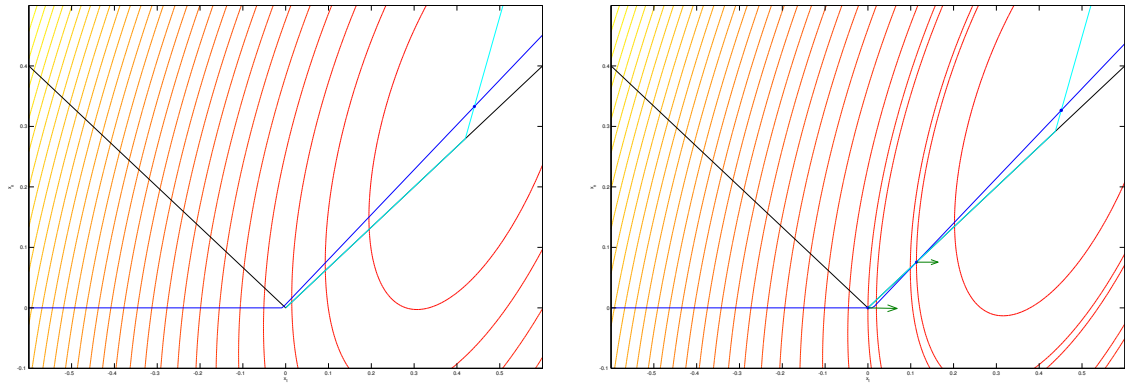

(a) Solution space of an impulse-velocity time-stepping LCP without a force-acceleration solution but only an impulsive solution.

(b) Solution space of an impulse-velocity time-stepping LCP with multiple solutions.

Figure 3: Solution spaces of impulse-velocity time-stepping LCPs.

5 CONTACT COMPLIANCE

As we saw in the previous sections we are able to remove the inconsistency but not the indeterminacy. The inconsistency is due to the inability of the force-acceleration approach to produce impulsive solutions. Shen and Stronge describe this jamming or self-locking process of the Painlevé paradox in [9] as follows: "The equations of motion bring a negative normal relative acceleration across the contact region due to a large rotational acceleration which is caused by a large friction force." They conclude that this is incompatible with force-acceleration complementarity conditions demanding non-negative accelerations. However, one can also argue in favor of the "shock assumption": To counteract the initially negative normal relative acceleration at the contact the normal reaction must increase. Increasing the normal reaction also increases the friction limit. This in turn implicates a stronger frictional reaction causing again an increase in rotational acceleration and consequently a negative normal relative acceleration at the contact requiring a stronger normal reaction. Note that there is no way (in a force-acceleration scheme) the frictional reaction can change the contact state at the time and thus the frictional reaction will always be at its limit. This iteration can either converge (for moderate friction) or diverge (for strong friction) for the paradoxical cases. The only way out of this loop in the divergent case is to allow a frictional *impulse* which can change the dynamic to a static contact. The frictional reaction then no longer increases with the friction limit.

The indeterminacy of the contact reactions is often ignored. If no friction is present then the velocity solution and thus the trajectories are the same for all feasible contact reactions. But as soon as dissipation occurs the velocity solutions also differ. The Painlevé paradox does already demonstrate that. In the case of non-unique solutions the solutions have different contact states and different energies. However, the problem gets more pronounced as soon as redundant constraints are involved [12, 6]. As an example consider a table sliding down a ramp. The problem is overconstrained and has one degree of freedom on how to distribute the contact reactions to the legs of the table. This can be used to generate considerably different outcomes even with small coefficients of friction. The indeterminacy due to redundant constraints is attended by a rank-deficient constraint Jacobian $\mathbf{J}$. This indeterminacy (at least for the discrete time-stepping problems) can be removed by introducing compliance at the contacts and driving the stiffness and damping coefficients towards infinity [7]. When adding compliance the system can still be formulated in terms of

complementarity conditions but the system matrix is then always positive definite (PD) instead of possibly positive semi-definite. But when considering true Coulomb friction indeterminacy can still occur even if the system matrix is PD as in the case of the Painlevé paradox.

When adding compliance to the contacts impulsive solutions can no longer occur. The system can then be described by discontinuous ordinary differential equations (ODE) of second order

$$\begin{pmatrix} m & & \\ & m & \\ & & I \end{pmatrix} \begin{pmatrix} \ddot{q}_x \\ \ddot{q}_y \\ \ddot{\varphi} \end{pmatrix} = \begin{pmatrix} f_x \\ f_y \\ \tau \end{pmatrix} + \mathbf{J}^T \boldsymbol{\lambda}, \tag{21}$$

where $\boldsymbol{\lambda}$ are forces specific to the choice of the compliance. When choosing a spring-damper for the normal reaction and a damper for the frictional reaction, $\boldsymbol{\lambda}$ reads

$$\begin{aligned} \lambda_n &= \begin{cases} 0 & \text{if } g_n > 0 \\ -k_n g_n - \gamma_n \min(\dot{g}_n, 0) & \text{else} \end{cases} \\ \lambda_t &= -\frac{\dot{g}_t}{\|\dot{g}_t\|_2} \min(\mu\lambda_n, \gamma_t \|\dot{g}_t\|_2). \end{aligned} \tag{22}$$

Such an ODE has a unique solution [9] for arbitrary (large) constants k_n, γ_n and γ_t. The model is simpler than the Kelvin-Voigt model used in [10] but also recovers true static contacts in the stiff limit. Note that the normal damping force is limited to approaching velocities, which ensures that normal reactions cannot be adhesive overall.

5.1 Solution Non-Existence Continued

Numerically solving the system of ODEs of the inconsistent Painlevé paradox from Sec. 2.1, 3.1 and 4.1 with Matlab's `ode45` integrator yields the results in Fig. 4. The figure has solutions for two different sets of constants. The solution, in contrast to the solution of Sec. 3.1, has a short period of initial sliding instead of an immediate impulse switching to a static contact. As soon as λ_t reaches its peak value the contact switches its state from a dynamic to a static contact until the contact breaks soon after. When increasing the stiffness the contact duration shortens and the reaction forces λ_n and λ_t get stronger. The integration ends soon after the contact opens.

Fig. 5(a) lists the integrals of the reaction forces until the contact breaks for the constants αk_n, $\alpha\gamma_n$ and $\alpha\gamma_t$ with varying α and $k_n = \gamma_n = \gamma_t = 1$. Fig. 5(b) plots the force integrals including the contact reaction $\boldsymbol{\Lambda}_2 = \boldsymbol{\Lambda}$ predicted by the instantaneous impulse-velocity LCP and the contact reaction $\delta t\tilde{\boldsymbol{\lambda}}$ predicted by the time-stepping scheme. One can see that the force integrals converge for increasing stiffnesses to the instantaneous impulse-velocity solution $\boldsymbol{\Lambda}$.

5.2 Solution Non-Uniqueness Continued

Repeating the same for the Painlevé paradox with multiple solutions from Sec. 2.2, 3.2 and 4.2, the force integrals converge to $(0, 0)^T$ when increasing the stiffness. Note that this does not depend on initial interpenetration being present or not.

6 CONCLUSION

The system of ODEs for rigid body dynamics with compliance always has a unique solution. As the examples above indicate, the reaction force integrals can converge to the reactions predicted by the time-stepping and instantaneous impulse-velocity complementarity problems in the stiff limit. The exact details are vague though. A thorough singular perturbation analysis of the system with contact compliance is necessary. Possibly the model has to be adapted to recover the impulse-velocity complementarity solutions in the limit in general. We expect the stiff limit to depend on k_n, γ_n and γ_t. Different ratios might produce different limit points explaining the indeterminacy.

Differentiating position constraints, as it was done in Sec. 2 and Sec. 3, and keeping the complementarity $\perp$ is controversial. Chatterjee argues in [2] that the complementarity in the velocity Signorini conditions is artificial. Removing the complementarity between the inequalities can lead e.g. to convex quadratic programming problems with unique solutions [1]. However, the solutions come along with non-zero restitution for sliding contacts. Keeping the complementarity corresponds to requiring inelastic collisions. Chatterjee gives the example of a rod protruding the edge of a table. When hitting the tip of the rod with a hammer at the free end a non-zero normal reaction is typically produced at the other end of the rod due to the flexion while at the same time it starts to lift off the table. This violates the velocity Signorini condition. This solution potentially arises in the stiff limit when modelling the rod with a torsion spring [11]. The solution predicted by the LCPs is recovered if the torsion spring stiffness is stronger than the stiffness of the table. However, this is typically not the case in experiments. This indicates that the LCP formulations as presented above stem from a stiff limit of a system of ODEs where contact compliance is added but no deformations take place in the interior of the objects as it is the case e.g. in collisions of hard spheres [3]. The numerical convergence studies in Sec. 5 also support this.

To remedy the indeterminacy Painlevé proposed [4]: "Two rigid bodies which under given conditions would not produce any pressure on one another, if they were ideally smooth, would likewise not act on one another if they were rough." Thus in the non-unique cases with a single contact we should always choose the reaction $(0, 0)^T$ if available. Again the numerical convergence study of the non-unique case in Sec. 5 supports this.

REFERENCES

[1] M. Anitescu. Optimization-based simulation of nonsmooth rigid multibody dynamics. *Math. Program.*, 105(1):113–143, 2006.

[2] A. Chatterjee. On the Realism of Complementarity Conditions in Rigid Body Collisions. *Nonlinear Dynamics*, 20:159–168, 1999.

[3] R. Cross. Differences between bouncing balls, springs, and rods. *American Journal of Physics*, 76(10):908–915, 2008.

[4] F. Génot and B. Brogliato. New Results on Painlevé Paradoxes. *European Journal of Mechanics - A/Solids*, 18(4):653 – 677, 1999.

[5] P. Painlevé. Sur les lois du frottement de glissement. *C. R. Acad. Sci. Paris*, 121:112 – 115, 1895.

[6] T. Preclik. Elastic Collisions in Complementarity-based Time-stepping Methods. Technical report, Friedrich-Alexander University Erlangen-Nuremberg, December 2010.

[7] T. Preclik, C. Popa, and U. Rüde. Regularizing a Time-Stepping Method for Rigid Multibody Dynamics. In *Proceedings of Multibody Dynamics 2011 (ECCOMAS Thematic Conference)*, 2011.

[8] T. Preclik and U. Rüde. Solution Existence and Non-Uniqueness of Coulomb Friction. Technical report, Friedrich-Alexander University Erlangen-Nuremberg, November 2011.

[9] Y. Shen and W. Stronge. Painlevé paradox during oblique impact with friction. *European Journal of Mechanics - A/Solids*, 30(4):457 – 467, 2011.

[10] P. Song, P. Kraus, V. Kumar, and P. Dupont. Analysis of rigid body dynamic models for simulation of systems with frictional contacts. *Journal of Applied Mechanics*, 68:118–128, 2000.

[11] D.E. Stewart. Rigid-Body Dynamics with Friction and Impact. *SIAM Review*, 42(1):3 – 39.

[12] M. Wojtyra and J. Frączek. Joint Reactions in Overconstrained Rigid or Flexible Body Mechanisms. In *Proceedings of Multibody Dynamics 2011 (ECCOMAS Thematic Conference)*, 2011.

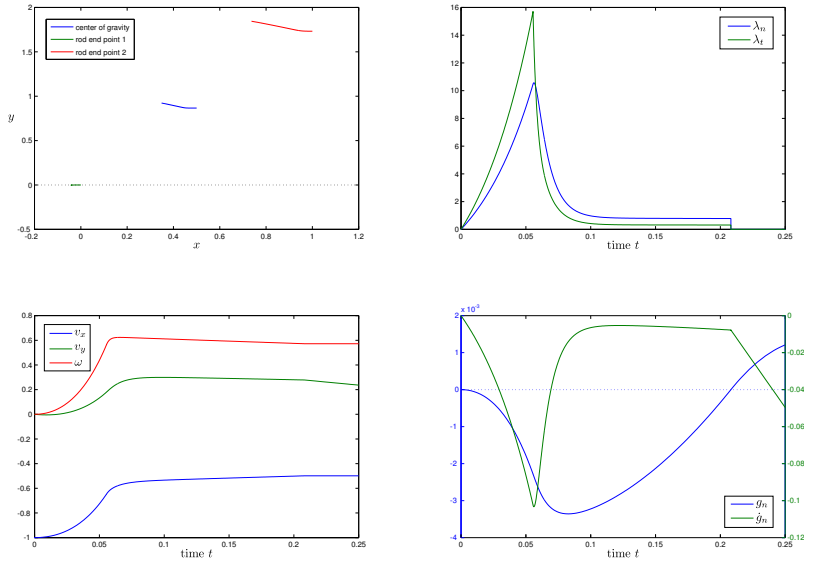

(a) The solution of the ODE with $k_n = \gamma_n = \gamma_t = 10^2$.

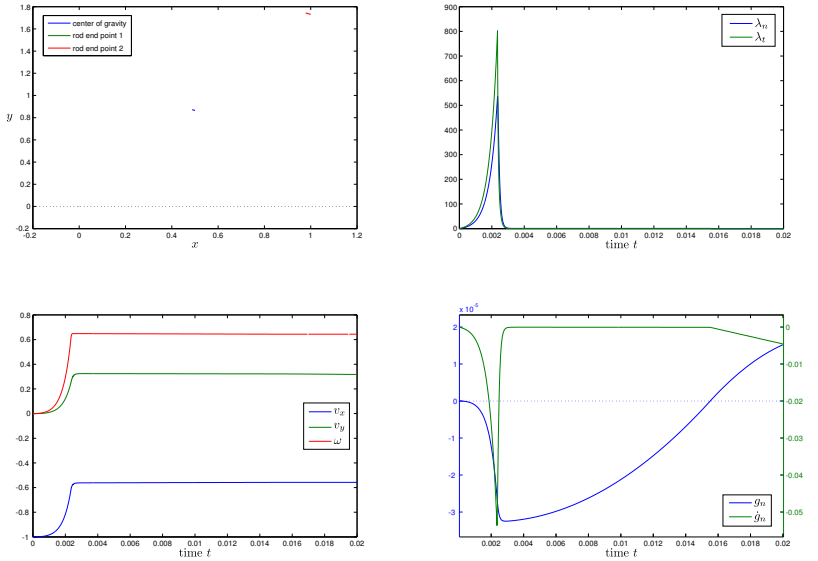

(b) The solution of the ODE with $k_n = \gamma_n = \gamma_t = 10^4$.

Figure 4: ODE solutions of the Painlevé paradox as presented in Sec. 2.1 having no solution with force-acceleration approaches.

α	10^3	10^4	10^5	10^6	10^7	10^8
$\int \lambda_n$	0.3688	0.3374	0.3285	0.3259	0.3251	0.3249
$\int \lambda_t$	0.4551	0.4426	0.4391	0.4380	0.4377	0.4376

(a) Numerical integration of contact reactions obtained from the time integration with varying α.

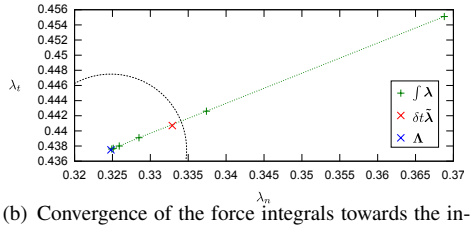

(b) Convergence of the force integrals towards the instantaneous impulse-velocity solution $\boldsymbol{\Lambda}$ for increasing α. The time-stepping solution $\delta t \tilde{\boldsymbol{\lambda}}$ is $\mathcal{O}(\delta t)$ off.

Figure 5: Contact force integrals until the contact breaks of the ODE solution of the Painlevé paradox as presented in Sec. 2.1.